

**Bioinspired composites from soft HEC matrix – strong effects of cellulose  
nanopaper reinforcement on viscoelastic behavior**

H Sehaquin, A Pei and LA Berglund

Wallenberg Wood Science Center and

Dept of Fiber and Polymer Technology

KTH

SE-100 44 Stockholm, Sweden

Abstract

Nanocomposites comprising materials from renewable resources are of great importance for ecological concerns. In this paper we used a filtration technique for the preparation of nanocomposites consisting of a soft HEC matrix surrounding nanofibrillated cellulose (NFC) that stack in the Z direction thus forming a hierarchical structure in a submicron scale. Thereafter, we investigate the role of NFC on mechanical, thermomechanical and creep properties of the resulting nanocomposites. The results show considerable improvement of these properties as a result of the formation of a strong percolated network of NFC in the polymer matrix as observed in the scanning electron microscope. Higher NFC loadings (>40%) were found to give synergetic properties with a higher strength and tree times increased toughness than that of the individual components. At high NFC loadings, the storage modulus of the

nanocomposites is increased by several orders of magnitude at elevated temperatures and is above 1 GPa at 200°C compared to 6MPa of the polymer matrix. Creep properties of the nanocomposites are found to be much superior than that of the matrix and approaches properties of composites used in aeronautical applications. All these results shows the attractive features of biomimetics for achieving high performance materials.

## **1. Introduction**

Sustainable activities are increasingly gaining importance nowadays due to their lesser environmental impacts. Practical examples are ecological housings in UK and renewable energy technologies in Denmark. The production and use of biocomposites plays a vital role in this line because of their biodegradability and the fact that they are totally or partially from renewable resources. Biocomposites refer to a multiphase system composed by a matrix and a reinforcement of natural fibers, the origin of natural fibers can be either vegetal or animal, cellulosic plant fibers are regarded as the most suitable fiber resource because of the large availability and ease of massive production. The matrix component in biocomposites can be synthetic or a bioplastic. When the latter is used as a matrix system, the biocomposites are called natural biocomposites and their environmentally friendly character is usually more pronounced. Therefore, plant fibres based natural composites are among the materials generating the most interests in the twenty-first century. These have already big potential in packaging applications.

Cellulose is the main load bearing component in plants where it is present in a hierarchical structure. Young's modulus of cellulose crystals was determined by XRD

and was found to be as high as 134GPa<sup>1</sup>. Cellulose has been successfully used as reinforcing phase in composites. A famous example is wood plastic composites (WPC) that have a big market in decking and fences in the united states<sup>2</sup>. WPC uses cellulose in the form of wood saw dust particles, and polyethylene, polypropylene and PVC as matrix systems. Cellulose based composites can also be made from plant fibers and generally biodegradable matrices such as starch, Polylactic acid and Polycaprolactones are preferred<sup>3</sup>.

Cellulose can also be used for nanocomposites fabrication when it is used in the form of nanofibrillated wood cellulose nanofibers (NFC)<sup>4</sup>, cellulose nanocrystals<sup>5</sup>, tunicate whiskers<sup>6, 7</sup> or bacterial cellulose nanofibers<sup>8</sup>. Nanofibrillated cellulose nanofibers are obtained from wood pulp fibers (or other plant fibers) after enzymatic<sup>9</sup> or chemical treatment<sup>10</sup> followed by a mechanical homogenization, and have a fibrillar morphology with a diameter of 5-30 nm and a length of several micrometers. Cellulose crystals are obtained after acid hydrolysis of wood or plant fibers and have a smaller diameter of about 5 nm but a shorter length of few hundred nanometers<sup>11</sup>. And bacterial cellulose is a form of cellulose nanofibers produced by bacteria such as acetobacter<sup>12</sup>. Cellulose nanocomposites show better performances than cellulose composites providing a good dispersion in the matrix. They also usually use a smaller content of reinforcement.

The last years have shown an increasing number of publications on cellulose nanocomposites, and characterization focus on structural analysis, mechanical and thermomechanical properties, thermal properties and optical properties. In the present study, we prepare cellulose nanocomposites using microfibrillated cellulose nanofibers (NFC) from wood and hydroxyl ethyl cellulose (HEC) matrix. High NFC loadings in HEC are prepared and the microstructure, mechanical, thermomechanical and creep

properties of the resulting nanocomposites are characterized. The present paper constitutes to our knowledge the first creep study of cellulose based nanocomposites.

## **Materials and methods**

### **1.1. Preparation of the nanocomposites**

NFC water suspension was prepared from softwood sulphite pulp fibers (Nordic Pulp and Paper, Sweden) according to a previously reported method by Henriksson et al.<sup>9</sup>. The pulp was first subjected to a pretreatment step involving enzymatic degradation and mechanical beating. Subsequently, the pretreated pulp was disintegrated by a homogenization process with a Microfluidizer M-110EH (Microfluidics Ind., USA), and a 2 wt% NFC suspension in water was obtained. HEC (average  $M_v = 1.300.000$  g/mol, substitution degree 1.5, molar substitution 2.5 ethylene oxide groups per anhydroglucose unit) was purchased from Sigma aldrich. The nanocomposites were prepared by first dissolving HEC in water using a magnetic stirrer overnight. The concentration of HEC solution obtained is 0.25wt%. The NFC is diluted from 2wt% to 0.25wt% by addition of water and stirring for 10min at 12000rpm in an Ultra Turrax mixer (IKA, D125 Basic). Different proportions of the HEC solution and NFC suspension corresponding to a total dry weight (NFC+HEC) of 450mg were mixed using a magnetic stirrer for one day. The mixture was degassed to remove bubbles and then vacuum filtrated on a glass filter funnel using a 0.65  $\mu\text{m}$  filter membrane, (DVPP, Millipore) according to a previously reported method for nanopaper<sup>13</sup>. The 0.65  $\mu\text{m}$  filter membrane does not allow NFC to go through it. At the end of the filtration, a wet cake is formed. The wet cake was stacked between metallic wire net and filter papers and then dried using a laboratory sheet drier (Rapid köthen) operating at 93 °C under a pressure of ca 100 mbar for 12 minutes. This resulted in NFC nanocomposites with a

thickness in the range of 65-80  $\mu\text{m}$ . After weighing the dry nanocomposite film, it was found that about 20% of the initial HEC amount used was lost through the filtrate. This may come from the low molecular weight fractions of the initial HEC.

Neat NFC film (NFC nanopaper) was prepared similarly by vacuum filtration of 160g NFC suspension at 0.25wt% until formation of a wet cake which is then dried at 93°C and 100 mbar for 12 minutes in a laboratory sheet drier (Rapid köthen).

The reference HEC film was prepared by solvent casting a previously degassed 100 ml HEC solution at 0.3wt% on a polystyrene petri dish under air atmosphere and room temperature.

All samples are conditioned at 50% relative humidity and 23°C for 1 week prior to mechanical testing.

### **1.2. Density measurements:**

Samples were dried in a dessicator containing silica drying agent for 2 days. Their dry weight is measured immediately after taken them from the dessicator. The density is calculated by dividing the dry weight of the sample by its volume, the volume is calculated from geometry of the films.

### **1.3. Water uptake at 50% relative humidity:**

Samples were dried in a dessicator containing silica drying agent for 2 days. Their dry weight is measured immediately after taken them from the dessicator. The samples are placed afterwards in a conditioning room at 50% relative humidity, and their weight is recorded at different time intervals. The water uptake at 50% relative humidity is taken at equilibrium once no more increase in the weight of the sample is observed.

### **1.4. Field-emission scanning electron microscopy (FE-SEM)**

The specimens were first dried in a dessicator overnight and then fixed on a metal stub using carbon tape and coated with a double-layer coating (ca 5 nm) consisting of graphite and gold–palladium using Agar HR sputter coaters. A Hitachi S-4800 scanning electron microscope operated at 1 kV was used to capture secondary electron images of the surface and cross-section of the samples.

### **1.5. Tensile mechanical properties**

Static tensile mechanical properties were tested on a universal material testing machine Instron 5566 equipped with a 500 N load cell. Specimen strips of 60 mm in length (distance between the clamps set to 30 mm), 5 mm in width, and a thickness in the range of 65–80  $\mu\text{m}$  were tested at 10%/min strain rate under a controlled relative humidity of 50% and a temperature of 23 °C. 3 specimens were tested per sample. Young's modulus was taken from the initial linear part of the stress-strain curve, the yield stress was taken from the intersection of the initial elastic region and the following plastic region. The work to fracture (toughness) was taken as the area under the stress-strain curve.

### **1.6. Dynamic mechanical thermal analysis (DMTA)**

Dynamic mechanical analyser (DMTA, TA Instruments Q800) was used in tension mode for the characterization of the thermomechanical properties of the specimens, samples geometry used is identical to the one used in static tensile test with the distance between clamps of ca 10mm. Temperature scans were performed with a heating rate of 5°C/min and a frequency of 1Hz from -50°C to 300°C under air atmosphere.

### **1.7. Creep test & modeling**

Creep test was performed using the Dynamic mechanical analyser (DMTA, TA Instruments Q800). Two samples were selected for this study, namely the HEC reference sample and the nanocomposite at 45% NFC loading, a static load of 10MPa was applied to the samples strips of similar geometry than those used for DMA. The test was performed under air atmosphere at various temperatures, namely 28, 80, 120 and 200°C for 10 hours. The creep recovery was recorded by unloading the samples for additional 10 hours.

A nonlinear viscoelastic model (Schapery model) was used to fit the creep behavior of the materials. The constitutive equation for the model is:

$$\text{Creep:} \quad \varepsilon(t) = \varepsilon_0 + \varepsilon_1 \cdot (1 - \exp(-t / \tau_1)) + c \cdot t^n \quad \text{Eq. 1}$$

$$\text{Creep recovery:} \quad \varepsilon_r(t) = \varepsilon'_0 + \varepsilon'_1 \cdot (1 - \exp(-\frac{t-t_r}{\tau'_1})) + c' \cdot (t-t_r)^n \quad \text{Eq. 2}$$

The elastic strain  $\varepsilon_0$  was taken as the strain immediately after applying the load.

## 2. Results and discussion

### 2.1. Density

Density of the composites of different weight fraction of NFC is shown in figure 1 and table 1. It can be seen that the experimental values (open circles) for the density of the composites fit relatively well with the line corresponding to no porosity in the composites, which means that the porosity of the composites is very low or absent. A deviation from this line is seen for the nanopaper sample, and this is because of the porosity it contains (about 10%). This porosity can be seen in the SEM images.

***Table 1: Density of NFC/HEC nanocomposites and reference materials***

%wt NFC	NFC volume fraction*	Density [kg m <sup>-3</sup> ]
0	0	1043
12	8	1081
38	29	1289
56	44	1332
68	59	1359
100	100	1377

\* calculated by taken 1550kg/m<sup>3</sup> for the density of NFC and 1050kg/m<sup>3</sup> for the density of HEC

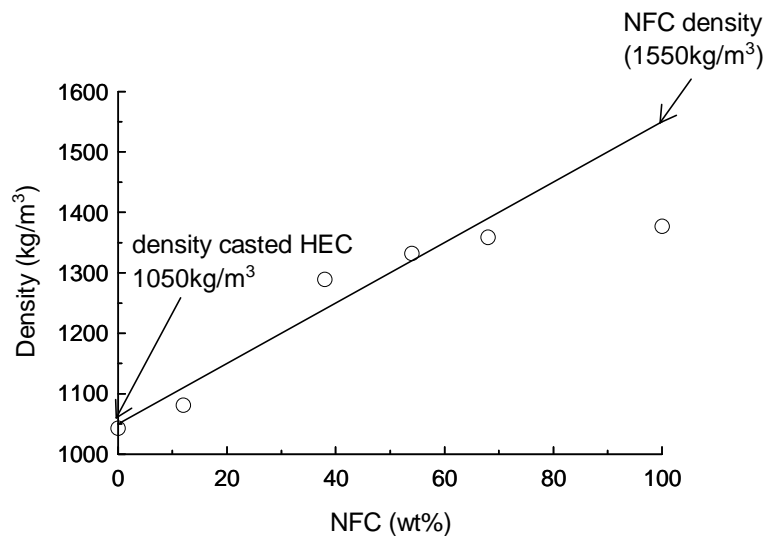


Fig. 1: Density of NFC/HEC nanocomposites and reference materials. Open circles are experimental values and continuous line correspond to no porosity.

## 2.2. Microstructure

Fig. 1 shows the microstructure of the surface of the nanocomposite and the reference NFC sample. In all samples, a percolated network formed by NFC can be seen. This network shows high interconnection degree of the nanofibrils which results from their high surface area and high aspect ratio. NFC sample showed apparent pores of ca 10nm while these pores tend to be replaced by HEC for the nanocomposites. No phase

separation in the nanocomposite sample surface could be observed due to the good molecular compatibility between the HEC and MFC. This good compatibility was also observed in the NFC / HEC water mixture that is stable upon storage. This feature is of key importance in the present nanocomposites since it allows during filtration the stacking of the nanofibrils surrounded by HEC macromolecules thus mimicking the primary cell wall of plants structure.

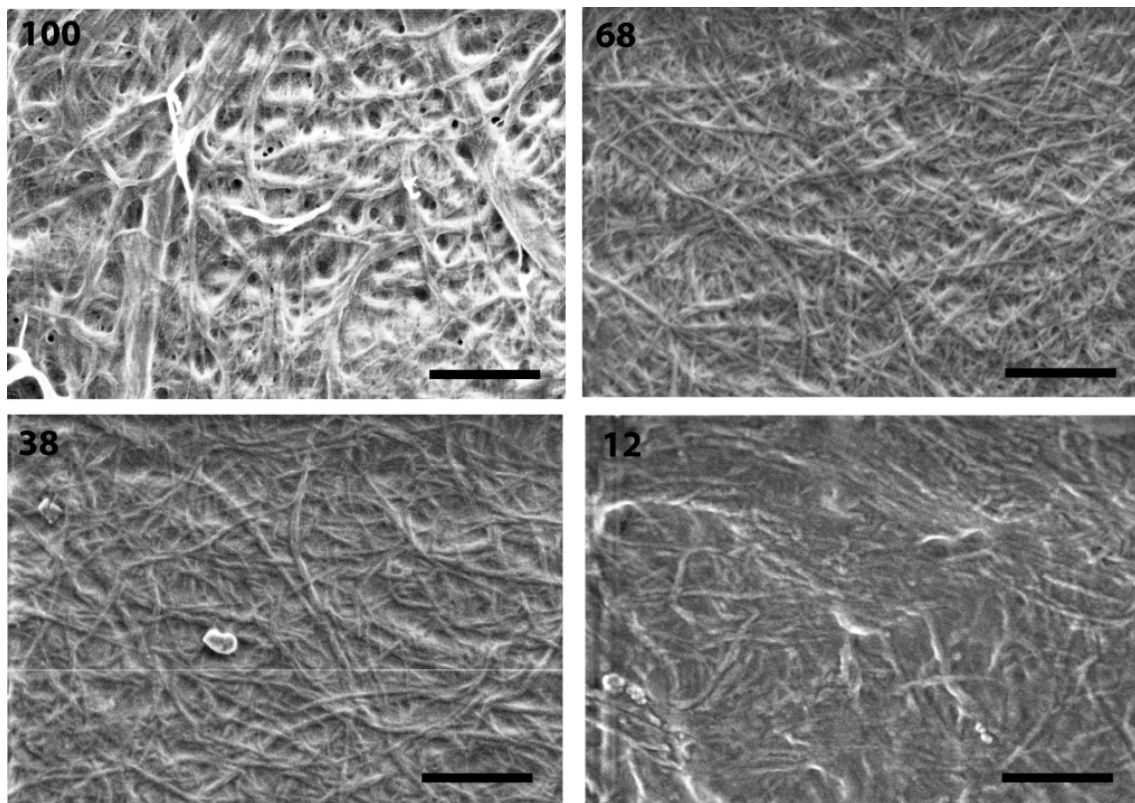


Fig. 2: SEM of the surface of the NFC sample and NFC / HEC nanocomposites. Numbers in the pictures represents NFC percentage. Scale bare is 500nm.

Fractured surfaces of the samples shows the embedding NFC network in the HEC matrix in a nacre like structure. NFC sample showed entangled nanofibrils stacking in a sheet like structures which is typical of samples prepared by filtration. In the nanocomposites at 68% MFC, The sheet like structure can still be seen as well as soft

HEC domains bonding interfibrils sheets (see arrow). This illustrates the structural hierarchy of the present materials in a submicron scale which is important for materials property enhancement. At high percentages of HEC in the nanocomposites (pictures 38 and 12), the domains between the sheetlike structures can no longer be discernible as they become filled by HEC.

The present filtration method for the preparation of hierarchical structures is a simple method. Here the choice of the polymer matrix is key to consider for the elaboration of such structure. This polymer should be compatible with cellulose and preferably of high molecular weight so that its interaction with the nanofibrils is increased and its probability to be filtrated away is reduced. Other polymer matrices were found to be less favorable for preparation with the present technique.

Preparation methods of hierarchical structure reported in the literature comprises the lbl, spin coating technique, and doctor blading. The present filtration method has the advantage of being simple, furthermore, it is solvent free and allows preparation of thick (100um), flat and smooth samples.

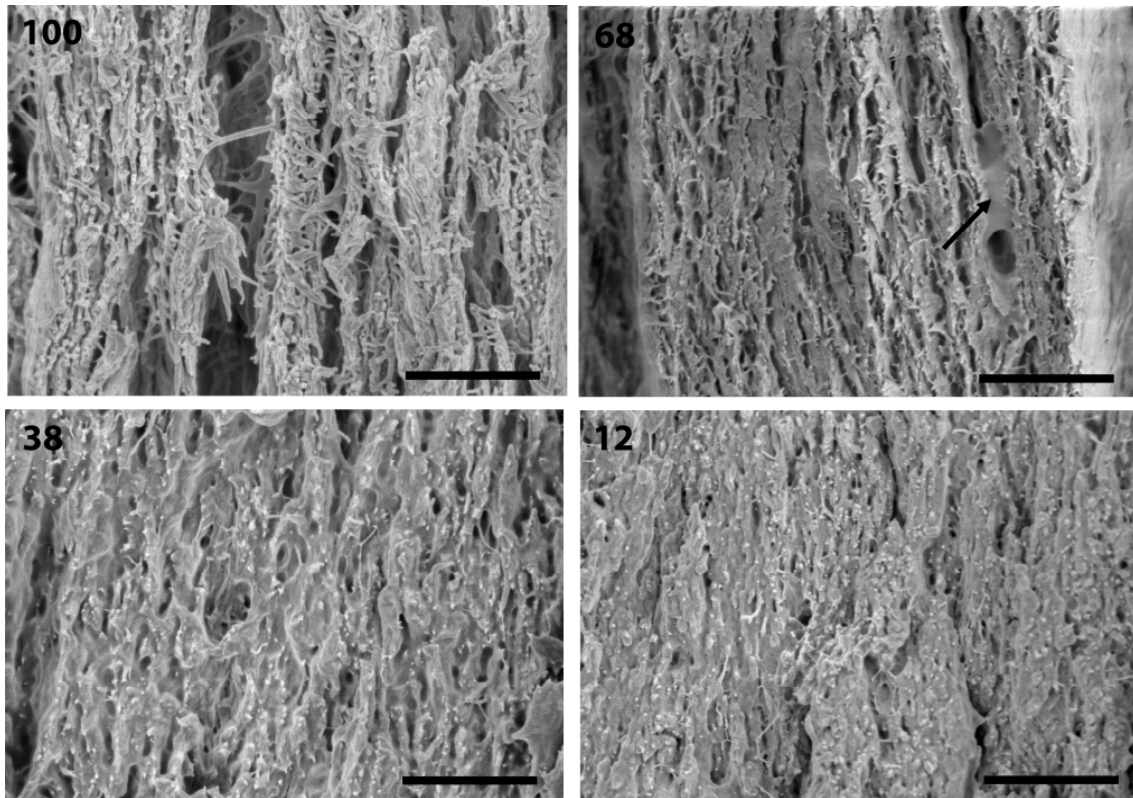
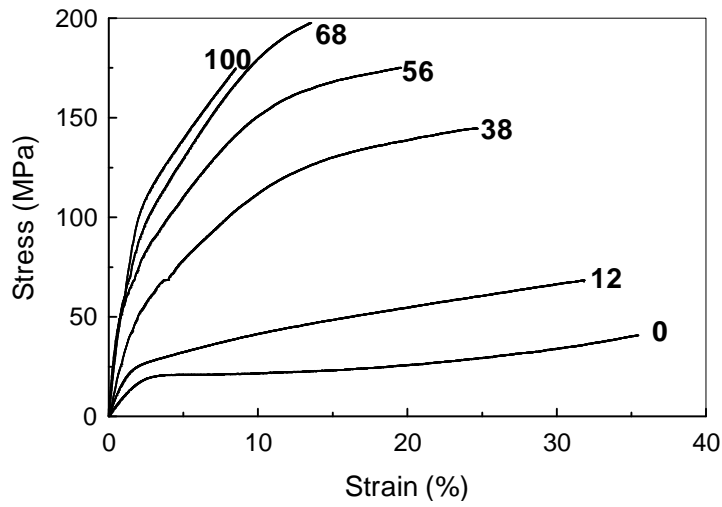


Fig. 3: SEM of fractured surfaces of NFC sample and NFC / HEC nanocomposites. Numbers in the pictures represents NFC percentage. Scale bare is 1 $\mu$ m.

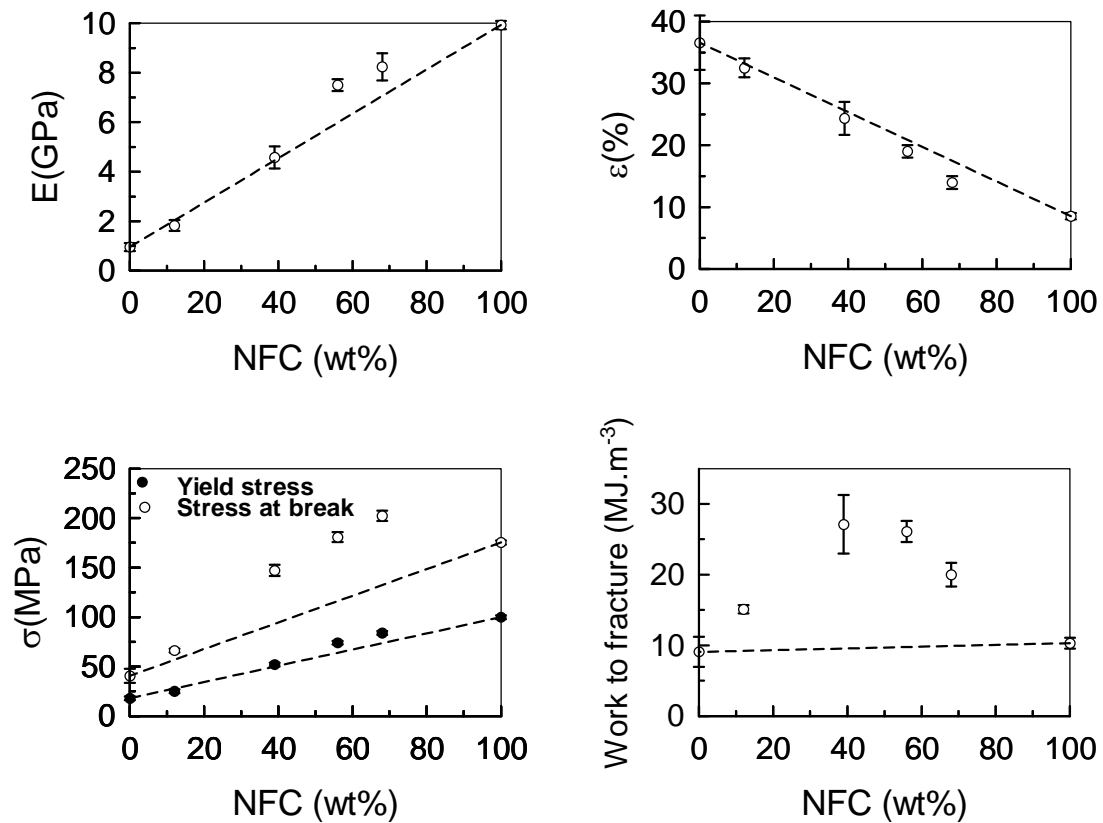
### 2.3. Tensile mechanical properties

The excellent mechanical properties of the NFC films (also termed nanopapers) has already been reported<sup>13</sup>. These come from the extensive hydrogen bonds and physical entanglements occurring among the nanofibrils. It was also seen a remarkable effect of HEC coatings onto bacterial cellulose nanofibers on the composites strength<sup>14</sup>. The present study aimed at investigating the combined effect of the strong NFC network with the ductile behavior of the HEC matrix especially at high NFC loadings and using the filtration method. Tensile stress-strain curves of the nanocomposites and the reference HEC and NFC samples are shown in Figure 3. Figure 4 and table 1 summarizes tensile mechanical properties.



**Figure 4: Stress strain curves of NFC/HEC nanocomposites and reference material.**

*NFC percentages are displayed next to the curves*



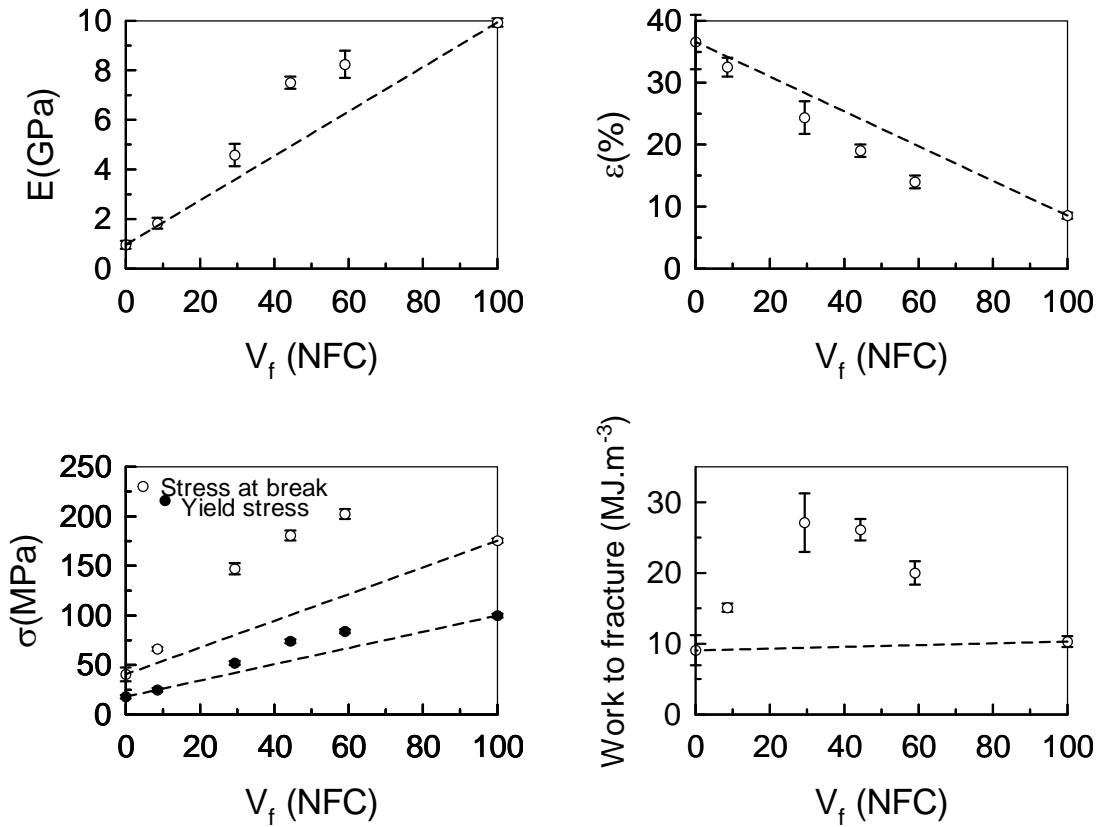


**Figure 5: Tensile mechanical properties of the nanocomposites and reference samples**

**Table 2: Mechanical properties of NFC/HEC nanocomposites and reference materials**

wt% NFC	Volume fraction NFC	Young's modulus [GPa]	Tensile strength [MPa]	Yield Stress [MPa]	Strain to failure [%]	Work to fracture [ $\text{MJ.m}^{-3}$ ]
0	0	0.95 (0.16)	41 (7)	18	36.6 (4.4)	9.1 (2.1)
12	5	1.87 (0.22)	66 (2)	25	32.5 (1.5)	15.1 (0.6)
38	20	4.58 (0.45)	147 (6)	52	24.4 (2.6)	27.1 (4.1)
56	32	7.50 (0.24)	181 (5)	74	19.0 (1.0)	26.1 (1.5)
68	46	8.23 (0.55)	202 (5)	84	14.0 (1.0)	20.0 (1.7)

100	100	9.93 (0.17)	175 (2)	100	8.5 (0.5)	10.3 (0.7)
-----	-----	----------------	---------	-----	--------------	---------------

- 2 distinct regions for NFC sample as reported by Henriksson et al. (elastic – plastic)
- 3 distinct regions for nanocomposites especially at high loadings (elastic – plastic - plastic) (plastic for HEC linking domains and plastic for MFC/HEC networks?)

The reference HEC and MFC samples have a strain to failure of 36.6% and 8.5% respectively. Nanocomposites strain to failure was found to follow a rule of mixture. Other tensile properties were found to deviate from the ROM towards positive synergetic effect. Especially at higher loadings (>38%), the stress at break of nanocomposites exceeded that of pure HEC by ca 5 times and were even higher than the pure NFC structure. These are due to the strong network formed by nanofibrillated cellulose embedded in a soft HEC that do not impart the strong fibrils interconnection (fig. 1). In the present nanocomposites, the combination of high strength and high strain to failure compared to pure NFC network makes them of much higher toughness than their individual components with a maximum of 27 MJ/m<sup>3</sup> recorded at 38% NFC content (similar to the cell wall composition NFC/hemicelluloses = 1/3 reference wood chemistry Roger Rowell??). This toughness is ca 3 times higher than that of HEC and NFC samples (9 and 10 MJ/m<sup>3</sup> respectively).

In a study by Zimmermann et al., another cellulose derivative, hydroxypropylcellulose was found a good polymer matrix where NFC has a good reinforcing effect<sup>15</sup>. At 10% NFC loading, the modulus achieved for the HPC/NFC nanocomposites was doubled and was of 800MPa and the maximum strain to failure of 15%. In the present study, at 12%

NFC loading, the modulus is also doubled but the values for modulus, strength and strain to failure are twice that reported for HPC/NFC nanocomposites, and this makes the toughness of the present material much greater. The work to fracture of the present materials as determined from tensile test is found to be greater than that reported by Zhou et al. (11MJ/m<sup>3</sup>) for HEC/BC composites<sup>14</sup>, and also than 70% NFC reinforced starch matrix (9.4MJ/m<sup>3</sup>)<sup>16</sup>.

It has been shown in several other studies the reinforcing effect of cellulose on starch<sup>7, 16</sup>, PLA<sup>17</sup>, a copolymer of styrene and butyl acrylate<sup>18, 19</sup>, phenolic resin<sup>4</sup>, PU<sup>20</sup>, HEC<sup>14</sup>, PVA and HPC<sup>15</sup>. Some of these where high cellulose content is used (>70%) have shown a strength as high as 300MPa<sup>14</sup> and 400MPa<sup>4, 14</sup> but a relatively low strain to failure of 7% and 5% respectively. Others with low cellulose content of 10% have shown a strain to failure as high as 100%<sup>15, 18</sup> and a strength of 15MPa and 60MPa. A good toughness was thus found with the latter where tough PVA matrix was used together with NFC. In the present study, high NFC loadings gave a combination of strength and strain to failure above 150MPa and 15% respectively which makes a high toughness material, this is illustrated in the materials selection chart in figure 5. Other reported high toughness materials in the literature used inorganic platelets, these include Co-Al-Co<sub>3</sub> and Co-Cu-NO<sub>3</sub> / chitosan films (160MPa 5% strain to failure)<sup>21</sup>. Clay playtelets reinforced chitosan films are of the few reported materials in literature combining good strength and ductility (300MPa strength and 25% strain to failure) thus giving a very tough material<sup>22</sup>.

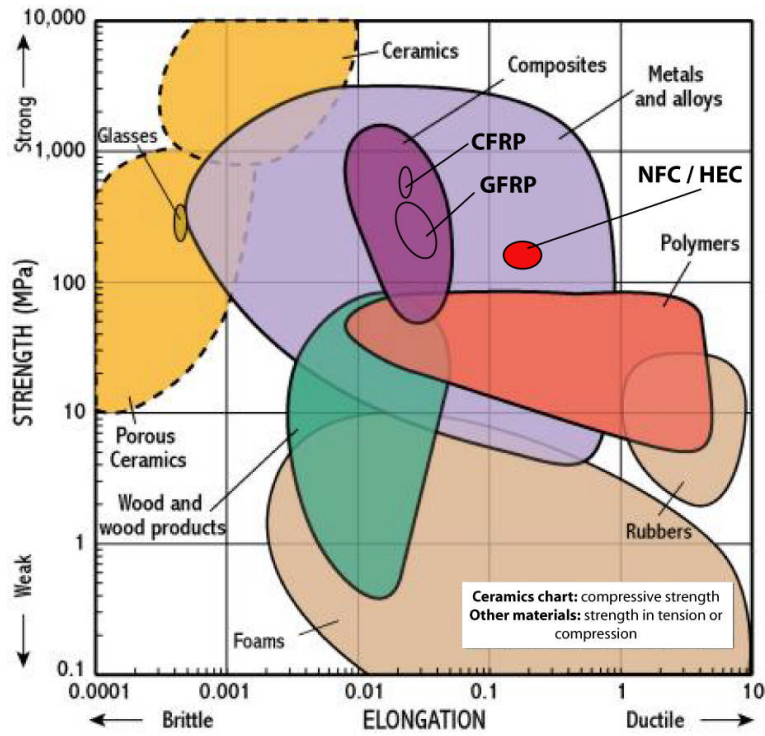


*Figure 6: Materials selection chart showing Strength – Elongation diagram.*

*NFC/HEC composites of high NFC loadings are represented in red.*

#### 2.4. Water uptake at 50% RH

Water uptake for composites and reference materials are shown in table 3. Figure 7 represents the kinetic of water absorption and figure 8 shows the water uptake at equilibrium. The HEC film is found to be more hygroscopic than NFC nanopaper, probably because HEC is amorphous while NFC is semi crystalline. Hygroscopy of the composites is found between that of HEC and NFC. It is also found that HEC absorbs water faster than NFC, while the composites show an intermediate behavior.

Table 3: water uptake of the composites and reference materials

% NFC	Water uptake at 50% RH (%)
-------	----------------------------

0	7.6
12	7.4
38	7.0
56	6.9
68	6.7
100	6.1

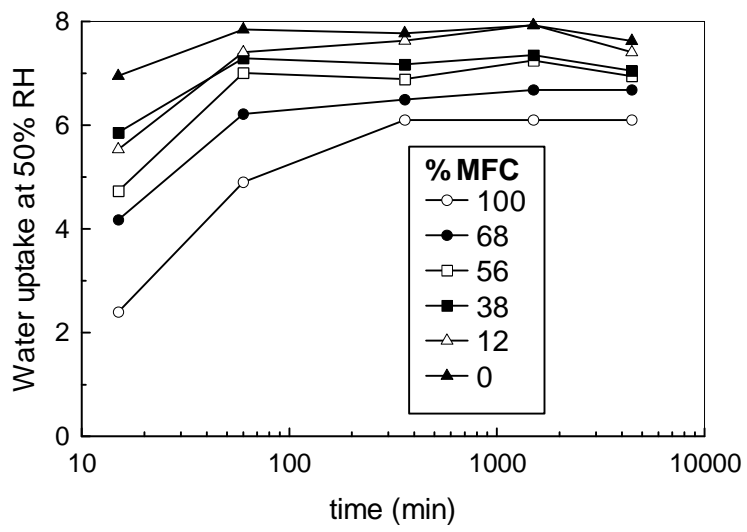


Figure : kinetic of water absorption kinetic for composites and reference materials

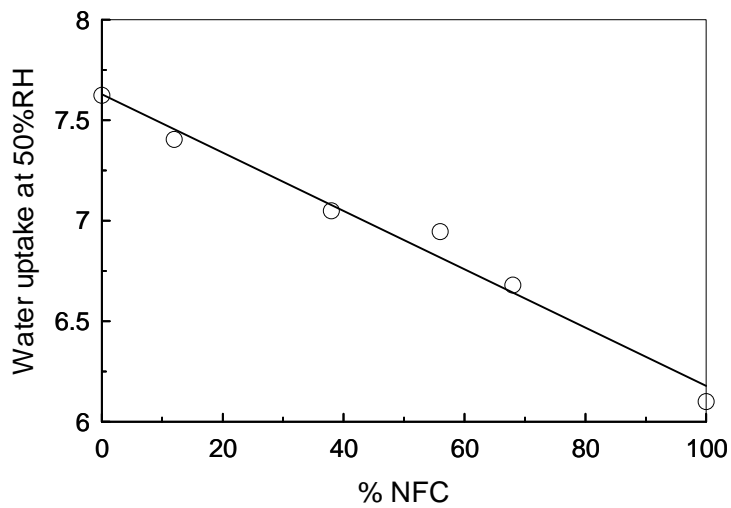
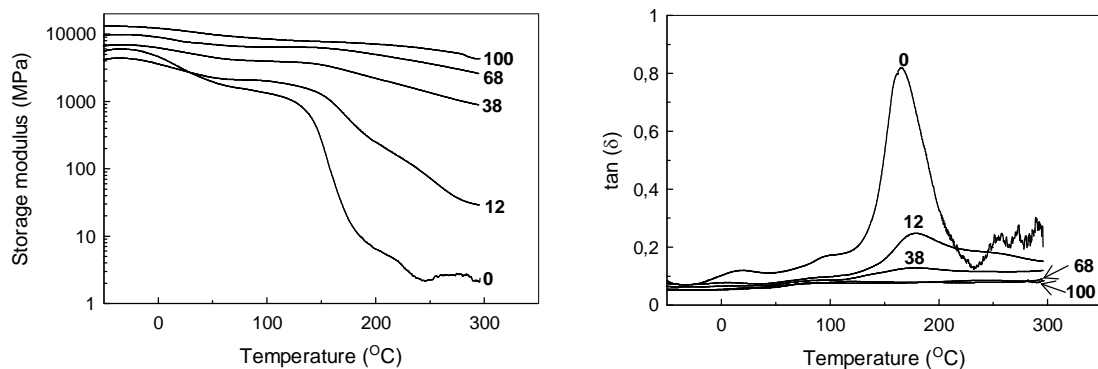


Figure 8: water uptake at equilibrium for the composites and reference materials

## 2.5. Thermomechanical properties

Figure HEC see its mechanical properties falling by several orders of magnitude above 165°C ( $T_g$ ?). The NFC/HEC nanocomposites however are much more thermally resistant, as they keep their storage modulus above 1GPa at temperature as high as 300°C for high NFC loadings. The high thermal stability of the nanocomposites is a result of the excellent thermomechanical properties of the NFC interpenetrated network which prevent the HEC matrix from yielding. The storage modulus at 200°C is plotted against %NFC in fig 7. The introduction of 12%NFC to the nanocomposites enhances their storage modulus at 200°C by a factor of 40 (6.5MPa vs 250 MPa). at NFC loadings of 38% and above, the storage modulus is above 1GPa at temperature as high as 250°C which is about 3 orders of magnitude higher than the HEC matrix. Improvement on thermomechanical properties of NFC reinforced polymers has been shown in several studies<sup>17-19</sup>. The present nanocomposites materials used high NFC loading and therefore have higher storage modulus at high temperature (about 2 orders of magnitude higher). Tan delta peaks observed for the HEC at 20°C and 165°C are considerably reduced after addition of NFC.



**Figure 9: Thermomechanical properties of NFC/HEC nanocomposites and reference materials**

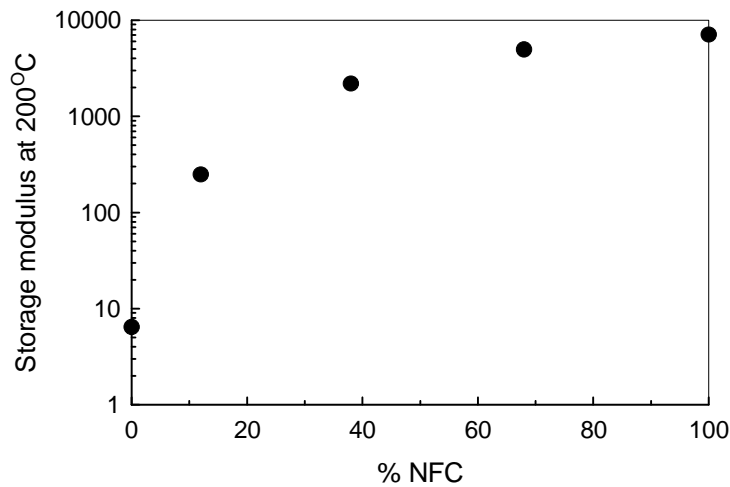


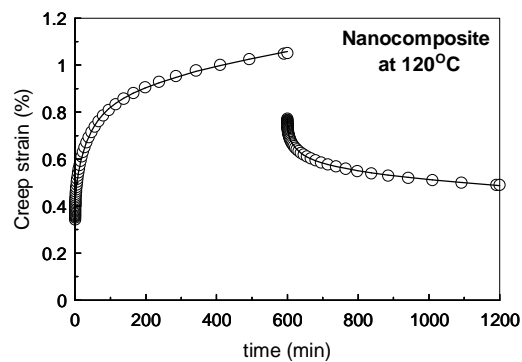
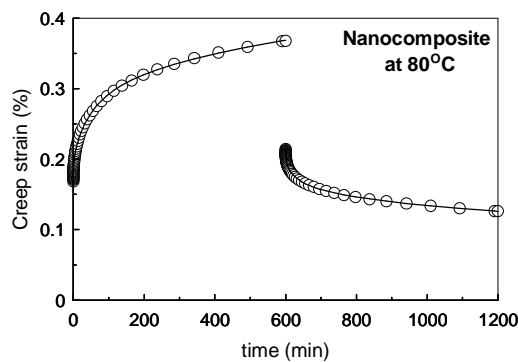
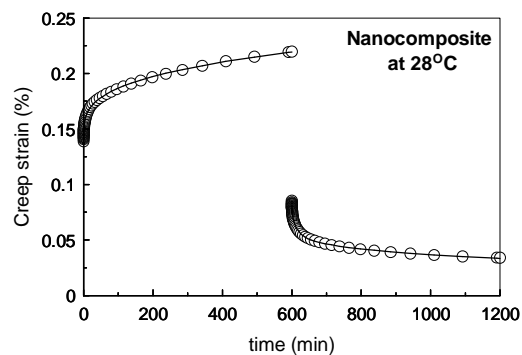
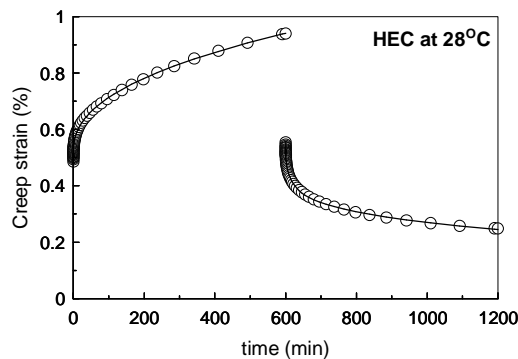
*Figure 10: Storage modulus at 200°C for NFC/HEC nanocomposites and reference materials*

## 2.6. Creep tests

Even though many publications have treated cellulose based nanocomposites, none at our knowledge investigated their creep properties. This property is of significance for structural applications. Composite materials such as (CFRP), GFRP are heavily studied because of their uses in aeronautical applications. Creep properties of WPC are also investigated because these materials are sold with a warranty of several years, so the long term behavior is of big importance.

Creep properties of the nanocomposites having 45% of NFC (55% of HEC) are shown in figure 4, the nanocomposites show higher creep resistance properties than the matrix in all the temperatures tested. Above the glass transition of HEC, the HEC film massively creeps and breaks within the early minutes of the test. The nanocomposites however, although containing 55% of HEC observe excellent creep resistance and do

not break even at 200°C. This is due to the mechanically robust and thermally stable NFC network. The creep properties of the present nanocomposites are about one order of magnitude lower than carbon fiber/epoxy matrix composites having fiber volume fraction between 35 and 40%, but seem to be of similar creep properties at higher temperatures of 75°C<sup>23</sup>. However, it should be noted that the epoxy composites mentioned can be tested under much higher stress (496MPa) due primarily to their very high stiffness in the longitudinal direction provided by aligned carbon fibers. The present nanocomposites have nanofibrillated cellulose nanofibers dispersed randomly in the plane and show a plastic deformation at around 100MPa and break at a maximum stress of 250MPa. Future efforts should be done in fabrication of aligned cellulose nanofibers in polymer matrices.



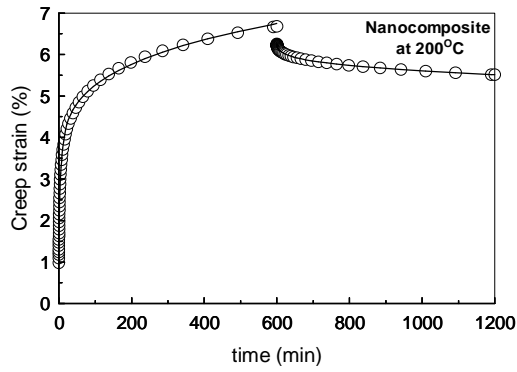


**Figure 11: Creep properties of 55%HEC/45%NFC nanocomposites and reference materials under 10MPa load. Open circles are experimental values, solid line correspond to the fitting)**

% NFC		$E_0$ [GPa]	$\epsilon_0$ [%]	<b>a</b>	<b>b</b>	<b>c</b>	<b>d</b>
HEC at 28°C	Creep	2.06	0.486	0.026	0.035	3.055	0.436
	Recovery	-	0.555	0.060	0.035	0.045	0.237
HEC/NFC at 28°C	Creep	7.19	0.139	0.010	0.004	0.470	0.313
	Recovery	-	0.085	0.010	0.012	0.063	0.215
HEC/NFC at 80°C	Creep	5.94	0.168	0.022	0.037	0.018	0.313
	Recovery	-	0.214	0.014	0.009	0.032	0.270
HEC/NFC at 120°C	Creep	2.92	0.343	0.083	0.164	0.027	0.296
	Recovery	-	0.773	0.045	0.037	0.036	0.267
HEC/NFC at 200°C	Creep	1.02	0.984	1.097	1.228	0.125	0.222
	Recovery	-	6.252	0.071	0.043	0.033	0.357

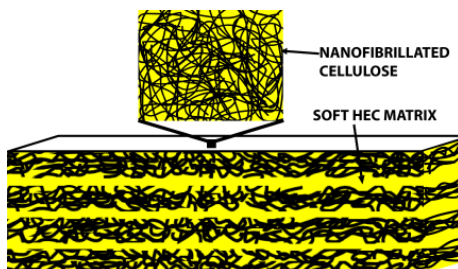
## Conclusion

The present study demonstrates the favorable characteristics of high volume fraction cellulose nanocomposites based on NFC networks. Hydroxyethyl cellulose (HEC) is used as a matrix, and is found to associate with cellulose NFC in a favorable manner. FE-SEM micrographs indicate that a layered structure is formed. The main achievement is that the work of fracture of NFC/HEC can be as high as  $27 \text{ MJ/m}^3$ . This is twice the value for the best NFC nanopaper. The main mechanism of deformation in the plastic region appears to be slippage of individual fibrils with respect to each other.

## Acknowledgments

Funding from the EU-project SustainComp and the KTH center Biomime is gratefully acknowledged.

## 3. DOI



## 4. References

1. Ichiro, S.; Yasuhiko, N.; Taisuke, I., Experimental determination of the elastic modulus of crystalline regions in oriented polymers. *Journal of Polymer Science* **1962**, 57, (165), 651-660.
2. Clemons, C., Wood-plastic composites in the United States - The interfacing of two industries. *Forest Products Journal* **2002**, 52, (6), 10-18.

3. Mohanty, A. K.; Misra, M.; Hinrichsen, G., Biofibres, biodegradable polymers and biocomposites: An overview. *Macromolecular Materials and Engineering* **2000**, 276, (3-4), 1-24.
4. Nakagaito, A. N.; Yano, H., The effect of morphological changes from pulp fiber towards nano-scale fibrillated cellulose on the mechanical properties of high-strength plant fiber based composites. *Applied Physics a-Materials Science & Processing* **2004**, 78, (4), 547-552.
5. Cao, X. D.; Habibi, Y.; Lucia, L. A., One-pot polymerization, surface grafting, and processing of waterborne polyurethane-cellulose nanocrystal nanocomposites. *Journal of Materials Chemistry* **2009**, 19, (38), 7137-7145.
6. Angles, M. N.; Dufresne, A., Plasticized starch/tunicin whiskers nanocomposites. 1. Structural analysis. *Macromolecules* **2000**, 33, (22), 8344-8353.
7. Angles, M. N.; Dufresne, A., Plasticized starch/tunicin whiskers nanocomposite materials. 2. Mechanical behavior. *Macromolecules* **2001**, 34, (9), 2921-2931.
8. Yano, H.; Sugiyama, J.; Nakagaito, A. N.; Nogi, M.; Matsuura, T.; Hikita, M.; Handa, K., Optically transparent composites reinforced with networks of bacterial nanofibers. *Advanced Materials* **2005**, 17, (2), 153-+.
9. Henriksson, M.; Henriksson, G.; Berglund, L. A.; Lindstrom, T., An environmentally friendly method for enzyme-assisted preparation of microfibrillated cellulose (MFC) nanofibers. *European Polymer Journal* **2007**, 43, 3434-3441.
10. Saito, T.; Kimura, S.; Nishiyama, Y.; Isogai, A., Cellulose nanofibers prepared by TEMPO-mediated oxidation of native cellulose. *Biomacromolecules* **2007**, 8, (8), 2485-2491.
11. Beck-Candanedo, S.; Roman, M.; Gray, D. G., Effect of reaction conditions on the properties and behavior of wood cellulose nanocrystal suspensions. *Biomacromolecules* **2005**, 6, (2), 1048-1054.
12. Iguchi, M.; Yamanaka, S.; Budhiono, A., Bacterial cellulose - a masterpiece of nature's arts. *Journal of Materials Science* **2000**, 35, (2), 261-270.
13. Henriksson, M.; Berglund, L. A.; Isaksson, P.; Lindstrom, T.; Nishino, T., Cellulose nanopaper structures of high toughness. *Biomacromolecules* **2008**, 9, (6), 1579-1585.
14. Zhou, Q.; Malm, E.; Nilsson, H.; Larsson, P. T.; Iversen, T.; Berglund, L. A.; Bulone, V., Nanostructured biocomposites based on bacterial cellulosic nanofibers compartmentalized by a soft hydroxyethylcellulose matrix coating. *Soft Matter* **2009**, 5, (21), 4124-4130.
15. Zimmermann, T.; Pohler, E.; Geiger, T., Cellulose fibrils for polymer reinforcement. *Advanced Engineering Materials* **2004**, 6, (9), 754-761.
16. Svagan, A. J.; Samir, M.; Berglund, L. A., Biomimetic polysaccharide nanocomposites of high cellulose content and high toughness. *Biomacromolecules* **2007**, 8, (8), 2556-2563.
17. Iwatake, A.; Nogi, M.; Yano, H., Cellulose nanofiber-reinforced polylactic acid. *Composites Science and Technology* **2008**, 68, (9), 2103-2106.
18. Malainine, M. E.; Mahrouz, M.; Dufresne, A., Thermoplastic nanocomposites based on cellulose microfibrils from *Opuntia ficus-indica* parenchyma cell. *Composites Science and Technology* **2005**, 65, (10), 1520-1526.
19. Samir, M.; Alloin, F.; Paillet, M.; Dufresne, A., Tangling effect in fibrillated cellulose reinforced nanocomposites. *Macromolecules* **2004**, 37, (11), 4313-4316.
20. Seydibeyoglu, M. O.; Oksman, K., Novel nanocomposites based on polyurethane and micro fibrillated cellulose. *Composites Science and Technology* **2008**, 68, (3-4), 908-914.
21. Yao, H. B.; Fang, H. Y.; Tan, Z. H.; Wu, L. H.; Yu, S. H., Biologically Inspired, Strong, Transparent, and Functional Layered Organic-Inorganic Hybrid Films. *Angewandte Chemie-International Edition* **2010**, 49, (12), 2140-2145.
22. Bonderer, L. J.; Studart, A. R.; Gauckler, L. J., Bioinspired design and assembly of platelet reinforced polymer films. *Science* **2008**, 319, (5866), 1069-1073.

23. Goertzen, W. K.; Kessler, M. R., Creep behavior of carbon fiber/epoxy matrix composites. *Materials Science and Engineering a-Structural Materials Properties Microstructure and Processing* **2006**, 421, (1-2), 217-225.